suggested for the decomposition of the TMA:ammonia adduct in the absence of a surface.[19]

The desorption of CH_3D above 600 K may be indicative of a reaction between amino groups and methyl groups bonded to aluminum. However, since the silica substrate used in this study is made up of many compressed layers, it is important to consider that species desorbing from one surface could react with a functional group on an opposing surface before being pumped out of the chamber. As a result, it should be noted that methyl radicals in the gas phase have been observed by Squire[38] for the decomposition of TMA on surfaces above 600 K. If formed under the conditions of this study, such a species could react with ND_2 groups to produce the CH_3D associated with the high-temperature desorption state.

Summary

Our results suggest that the uptake of NH_3 is the specific result of Al-N bond formation on each of the TMA-derivatized surfaces used in this study. While the presence of aluminum is solely responsible for achieving this fundamental requirement for the nucleation of AlN precursors on silica, it is the presence of methyl groups bonded to aluminum that facilitates the irreversible incorporation of nitrogen on the surface in the form of bridging amino groups.

Ammonia reacts with a methylaluminum surface complex on silica at 300 K to form a methylaluminum:ammonia surface adduct. Two reaction pathways are available for the decomposition of this species at low temperatures. Reaction pathway one: From 300 to 600 K, at sufficiently high coverages, ammonia and methyl groups from adjacent adducts on the surface react together via an interadsorbate reaction mechanism yielding methane and Al-NH_2-Al bridging groups. In this way, ammonia directly hydrogenates methyl groups bonded to aluminum, decreasing the source of carbon contamination and increasing the number of Al-N bonds to the surface. Reaction pathway two: Above 300 K, cleavage of the Al-N bond in the adduct competes with the interadsorbate reaction mechanism. This results in the desorption of ammonia and a decrease in the number of Al-N bonds to surface. There does not appear to be an intraadsorbate decomposition mechanism available for the methylaluminum:ammonia surface adduct that leads to the retention of nitrogen on the surface.

Acknowledgment. Financial support for this work provided by the U.S. Department of Energy, Office of Basic Energy Sciences, Division of Materials Sciences, under contract DE-AC04-76DP00789 is gratefully acknowledged. We thank C. H. F. Peden and J. R. Creighton for their valuable comments. We also thank L. V. Interrante for allowing us to examine his vibrational spectrum of the dimethylaluminum-amide trimer $[(CH_3)_2AlNH_2]_3$ prior to its publication. The technical assistance provided by M. L. Thomas is noted with appreciation.

Registry No. TMA, 75-24-1; TMA:ammonia adduct, 20775-95-5; ammonia, 7664-41-7; silica, 7631-86-9; aluminum nitride, 24304-00-5.

(38) Squire, D. W.; Dulcey, C. S.; Lin, M. C. *J. Vac. Sci. Technol. B* **1985**, *3*, 1513.

Molecular and Supermolecular Origins of Enhanced Electronic Conductivity in Template-Synthesized Polyheterocyclic Fibrils. 1. Supermolecular Effects

Zhihua Cai, Junting Lei, Wenbin Liang, Vinod Menon, and Charles R. Martin*

Department of Chemistry, Colorado State University, Fort Collins, Colorado 80523

Received April 19, 1991. Revised Manuscript Received July 8, 1991

The pores in a nanoporous membrane can be used as templates for the synthesis of nanostructures. We have recently shown that conductive polymer fibrils, obtained via this "template" synthetic method, can show dramatically higher electronic conductivities than conventional versions of the analogous polymers. In this and a succeeding paper we explore the molecular and supermolecular origins of this enhanced electronic conductivity. This paper focuses on supermolecular effects. We have used dc and optical measurements of conductivity, X-ray diffraction, and polarized infrared absorption spectroscopy to show that the polymer chains in the narrowest template-synthesized fibrils are preferentially oriented parallel to the axes of these fibrils. This preferential polymer chain orientation is partially responsible for the observed conductivity enhancements.

Introduction

The pores in nanoporous membranes can be used as templates for the synthesis of nanostructures.[1-6] This approach has been used to produce nano cylinders,[4,5] fibers,[1,2] wires,[6] and hollow tubules.[3] We have coined the term "template synthesis" for this nanostructure fabrication process.[3] We have recently shown that when the template method is used to synthesize nanoscopic conductive polymer fibrils, electronic conductivities along the axes of these fibrils can be dramatically higher than conductivities of bulk forms of the analogous polymers.[1]

* Corresponding author. Part of this work was conducted at Texas A&M University.

(1) Cai, Z.; Martin, C. R. *J. Am. Chem. Soc.* **1989**, *111*, 4138.
(2) Liang, W.; Martin, C. R. *J. Am. Chem. Soc.* **1990**, *112*, 9666.
(3) Martin, C. R.; Van Dyke, L. S.; Cai, Z.; Liang, W. *J. Am. Chem. Soc.* **1990**, *112*, 8976.
(4) Tierney, M. J.; Martin, C. R. *J. Phys. Chem.* **1989**, *93*, 2878.
(5) Penner, R. M.; Martin, C. R. *J. Electrochem. Soc.* **1986**, *133*, 2206.
(6) Williams, W. D.; Giordano, N. *Rev. Sci. Instrum.* **1984**, *55* (3), 410.

0897-4756/91/2803-0960$02.50/0

Table I. Characteristics of the Nuclepore Membranes Used in These Studies

pore diam, nm		porosity[a]		
nominal[c]	measd[d]	nominal[c]	measd[d]	thickness,[b] μm
30	30 ± 7	0.0042	0.0046	7
50	50 ± 4	0.0059	0.0067	
100	78 ± 17	0.0233	0.015	8
200	150 ± 20	0.090	0.032	10
600	530 ± 50	0.085	0.064	
800	800 ± 70	0.140	0.140	10
1000		0.145		12

[a] Fractional pore area. [b] Measured by using a digital micrometer. [c] From Nucleopore Corp. product literature. [d] Measured from electron micrographs of the surfaces of the membranes.

Cahalane and Labes have observed a similar enhancement in conductivity for conductive polymer prepared via a derivative of the template method.[7]

We are currently exploring the genesis of this enhanced electronic conductivity. We have discovered that there are both molecular and supermolecular differences between template-synthesized conductive polymers and conventional forms of these polymers. We will show in this and a succeeding paper[8] that these molecular and supermolecular differences are responsible for the enhanced electronic conductivities of the template-synthesized materials. This paper focuses on the supermolecular structures of template-synthesized polyheterocyclic fibrils and on the effects of supermolecular structure on conductivity in these fibrils.

The unique supermolecular feature of template-synthesized conductive polymer fibrils is preferential polymer chain orientation.[2] We have used a combination of polarized infrared absorption spectroscopy,[2] dc and optical measurements of conductivity, and X-ray diffraction analyses to show that the polymer chains in narrow template-synthesized polyheterocyclic fibrils are preferentially oriented parallel to the axes of these fibrils. These and related results are presented here.

Experimental Section

Materials. Polypyrrole (PPY) and poly(3-methylthiophene) (PMT) were investigated in these studies. The starting materials, pyrrole and 3-methylthiophene (Aldrich, 99%), were twice-distilled under nitrogen, immediately prior to use. Purified water, obtained by passing house-distilled water through a Milli-Q (Millipore) water purification system, was used as the solvent for PPY synthesis. UV-grade acetonitrile (Burdick-Jackson) was used for the PMT syntheses. KBr was Aldrich IR grade. All other reagents were used as received.

Nuclepore microporous polycarbonate filters (Nuclepore Corp.) were used as the template membranes.[1,3,9] Nuclepore is available in a variety of pore diameters and densities. The specifications for the membranes used in these studies are shown in Table I. The nominal values for the pore diameters and densities were supplied by the Nuclepore Corp. The measured values were obtained from in-house electron microscopic analyses of these membranes.[9] Accurate values for pore diameter, pore density, and membrane thickness are required to calculate fibril conductivity.[1] We used our measured values (Table I) for these calculations. Nonporous polycarbonate sheet, similar to the sheet used to make Nuclepore membrane, was obtained from Mobay (Makrofol KG).

Polymer Syntheses. Two types of PMT and PPY were synthesized. The first was the fibrillar polymer, which was synthesized by using the Nucleopore membranes (Table I) as the template materials.[1,3] The second was a "powderous" version of the polymer. The powderous versions were synthesized under identical conditions as the fibrillar materials but without the use of the template membrane. The powderous versions serve as "controls" versus which the properties of the fibrillar materials were evaluated. Electrochemically synthesized film[10,11] was also used as a control material.

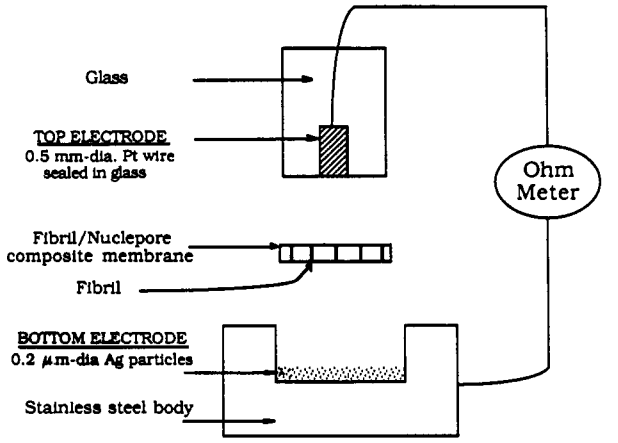

Figure 1. Schematic of apparatus used to conduct two-point conductivity measurements on the fibril/Nuclepore composite membranes.

Fibril synthesis was accomplished using the apparatus shown in Figure 1 of ref 3. The Nuclepore membrane separated the monomer solution from a solution of a chemical oxidant, which served as the polymerization agent. Unless otherwise noted, the monomer solution for PPY was 0.1–0.2 M aqueous pyrrole, and the oxidant was 2 M aqueous $FeCl_3$. For PMT, the monomer solution was 0.4–0.6 M 3-methylthiophene and the oxidant was 2–3 M $Fe(ClO_4)_3$ (solvent = acetonitrile). The Fe^{3+} was added to the outer compartment[3] first. The monomer solution was added to the inner compartment[3] 10–20 s later. Polymerization was allowed to proceed for 2 h. The membrane was then removed from the polymerization apparatus and rinsed with copious quantities of water or CH_3CN.

To investigate the effect of synthesis temperature on conductivity, some fibers were synthesized at low temperatures (0 and −20 °C). 50:50 methanol water was used as the solvent for these low-temperature syntheses. Polymerizations at these low temperatures were allowed to proceed for 6 h.

As indicated in our prior correspondences,[1-3] template synthesis yields conductive polymer fibrils, which run through the pores in the Nuclepore membrane, and thin polymer films, which coat both faces of the membrane. The fibrils can be isolated by dissolution of the Nuclepore; however, the surface layers must be removed prior to dissolution. The surface layers were removed by polishing both faces of the membrane with 0.05-μm alumina powder. After polishing, the fibril/Nuclepore composite was ultrasonicated in water to remove the alumina powder. The Nuclepore was then dissolved by immersion in stirred CH_2Cl_2. The fibrils were collected by filtration[12] and rinsed with copious quantities of CH_2Cl_2 to remove traces of polycarbonate.

The powderous (control) versions of PPY and PMT were prepared by simply mixing the monomer solution with a solution of the polymerization agent. The polymer formed as a fine black precipitate; this precipitate was stirred in the mother liquor for ca. 1 h and then collected by filtration. The polymer was then rinsed with copious quantities of either water or acetonitrile and dried in vacuo.

Dc Conductivity. Dc conductivity along the fibril axis was obtained by measuring the bulk resistance across the fibril/Nuclepore composite membrane.[1,2] Resistances were measured by

(7) Cahalane, W.; Labes, M. M. *Chem. Mater.* **1989**, *1*, 519.
(8) Cai, Z.; Liang, W. B.; Martin, C. R. Manuscript in preparation.
(9) Cheng, I. F.; Whiteley, L. D.; Martin, C. R. *Anal. Chem.* **1989**, *61*, 762.
(10) Yamaura, M.; Hagiwara, T.; Iwata, K. *Synth. Met.* **1988**, *26*, 209.
(11) Sato, M.; Tanaka, S.; Kaeriyama, K. *Synth. Met.* **1986**, *14*, 279.
(12) Van Dyke, L. S.; Martin, C. R. *Langmuir* **1990**, *6*, 1118.
(13) We initially used two Pt wires as the electrodes; however, unless the surfaces of these two solid electrodes were perfectly parallel, good contact with both faces of the membrane could not be achieved. The particle bed electrode obviates this problem because it is like a fluid and thus can conform to the lower membrane surface, regardless of angle.

Table II. Typical Raw Resistance Data for Several Fibril/Nucleopore Composite Membranes

polym[a]	fibril diam, nm	resistance,[b] Ω	
		doped	undoped
PPY	30	0.25	1400
PPY	200	0.14	2700
PPY	800	0.09	
PMT	30	0.17	1×10^6
PMT	200	0.24	
PMT	600	0.39	5×10^6

[a] Polymers were synthesized at 25 °C. [b] Background resistance noise was ±0.005 Ω.

using a two-point method based on the apparatus shown in Figure 1. Unless otherwise noted, the upper electrode was a 0.5-mm-diameter Pt wire sealed in glass. The lower electrode was a bed of 0.2-μm-diameter Ag particles.[13] The ohmmeter (Keithley 190) was calibrated by using high-precision resistors.

We initially completely removed the PPY or PMT surface layers prior to making resistance measurements on the fibril/Nuclepore composites. However, after removal of the surface layers, it proved impossible to obtain reproducible resistance data for the composite membrane. Better reproducibility was obtained when the surface layers were left intact. Clearly, the surface layers function as strongly adherent electrical contacts to the fibrils and thus minimize contact resistance problems.

While leaving the surface layers intact minimized contact resistance, it is in principle possible that the measured composite membrane resistance is a convolution of the resistances of the fibrils (wanted) and the resistances of these surface layers (unwanted). To circumvent this problem, we adopted the following compromise protocol: Rather than completely removing the surface layers, these layers were thinned by polishing with a laboratory tissue.[14] Electron microscopic analyses showed that after this (less abrasive) polish, the surface layers were less than 200 nm thick.[15] Appendix A shows that these ultrathin surface layers do not contribute to the membrane resistance.

A pressure of ca. 7×10^3 psi was applied between the upper and lower electrodes during the resistance measurements. This pressure was arrived at via a study of the effect of applied pressure on the measured resistance of the fibril/Nuclepore composite. An IR pellet press was used to control the applied pressure. The measured resistance initially decreased with pressure but then leveled at pressures above ca. 7×10^3 psi.[15] The higher resistance, at lower pressures, undoubtedly reflects a contribution from contact resistance. Because the measured resistance becomes independent of applied pressure, at high pressures, we assume (see below) that the contact resistance has been reduced to a negligible value.

Defining the electrode area presents another potential source of error (see Appendix A). We assume that the relevant area is just the area of the upper, Pt wire, electrode. If this is true, then a plot of measured resistance vs. the inverse of the electrode area should be linear, with zero intercept. Figure 2 shows that this is indeed the case.

Typical raw resistance data for several fibril/Nuclepore composites are shown in Table II. The conductivity along a single fibril can be calculated from these data (see Appendix B), provided the number and diameter of fibrils on the membrane are known (Table I). As a further test of the validity of our two-point method, we obtained analogous resistance data after chemically "undoping" the conductive polymer fibrils (Table II). Undoping was accomplished by exposing the membranes to 2 M NaOH (PPY)[16] or 0.2

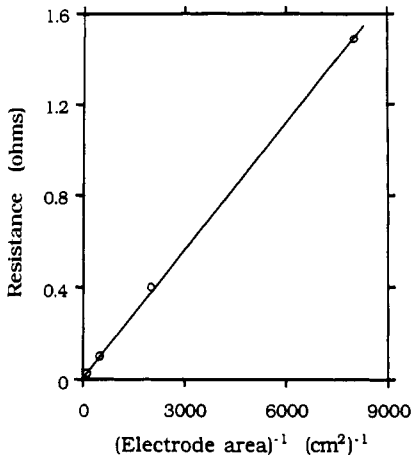

Figure 2. Plot of resistance of a fibril/Nuclepore composite membrane vs. inverse of area of (upper) Pt disk electrode (see Figure 1). The pore diameter in the membrane was 30 nm.

M $NaBH_4$ (in CH_3CN; PMT).[17] Because the undoped fibril is an electronic insulator,[16,17] the resistance of the composite membranes should increase dramatically. Table II shows that this is, indeed, the case.

Four-point measurements of electronic conductivity are preferable to two-point measurements. However, it is impossible to obtain four-point measurements in our nanoscopic fibrils. Contact resistance is the most significant problem in a two-point measurement. There are, however, other potential problems. For example, we assume that all of the pores are filled with contiguous conductive polymer fibrils. Furthermore, as indicated above, we assume that the resistances of the surface layers are negligibly small.

It is important to point out that if these assumptions are not correct—i.e., if contact resistance is not negligible or if some of the pores are devoid of fibrils or if the surface layers do contribute to the measured resistance—then the *real* fibril conductivities would be *higher* than the *measured* conductivities reported here. Hence, the dc conductivities reported here should be viewed as minimum values. Finally, it is important to point out that optical measurements of electronic conductivity (see below) corroborate the dc conductivities obtained from our two-point measurements.

Conductivities of the powderous polyheterocyclic samples were obtained by pressing the powders into pellets; a pressure of 2×10^6 psi was used. A standard four-point method was used to obtain the conductivities of the pressed pellets.[18] Conductivities for electrochemically synthesized films were taken from the literature.[11,12] The conductivities reported in these papers[11,12] are the highest conductivities reported for electrochemically synthesized PPY and PMT.

Optical Conductivity. As discussed by Chien, the infrared absorption spectrum for an electronically conductive polymer can be used to calculate an optical conductivity (σ_{opt}) for the polymer.[19] Such calculations make use of the Drude approximation.[20] A discussion of the assumptions involved in the Drude model can be found in refs 19–21. Briefly, the Drude model assumes that the free carriers (e.g., electrons in metals) absorb light and, because these carriers are also responsible for electronic conduction, this absorbance can be related to the electronic conductivity. The Drude model has been used to calculate σ_{opt} values for a variety

(14) A Kim-Wipe was wetted with water and each surface of the membrane was hand polished for several minutes. The surface of the Kim-Wipe darkened during polishing, indicating that polymer had been removed from the membrane. The membrane was then rinsed with copious quantities of water.

(15) These data are available upon request.

(16) Inganas, O.; Erlandsson, R.; Nylander, C.; Lundstrom, I. *J. Phys. Chem. Solids* **1984**, *45*, 427.

(17) When PMT is treated in this way, it losses the dark coloration characteristic of the doped polymer, and as indicated in Table II, the resistance increases dramatically.

(18) Penner, R. M.; Martin, C. R. *J. Electrochem. Soc.* **1986**, *133*, 310.

(19) Chien, J. C. W. *Polyacetylene*; Academic Press: New York, 1984; pp 551–552.

(20) Simon, J.; Andre, J. J. *Molecular Semiconductors*; Springer-Verlag: New York, 1985; pp 8–17.

(21) Abeles, F. *Optical Properties of Solids*; North-Holland: Amsterdam, 1972; pp 143–145.

(22) Yakushi, K.; Lauchlan, L. J.; Clarke, T. C.; Street, G. B. *J. Chem. Phys.* **1983**, *79*, 4774.

(23) Hasegawa, S.; Kamiya, K.; Tanaka, J.; Tanaka, M. *Synth. Met.* **1986**, *14*, 97.

(24) Fincher, C. R., Jr.; Ozaki, M.; Tanaka, M.; Peebles, D.; Lauchlan, L.; Heeger, A. J.; MacDiarmid, A. G. *Phys. Rev. B* **1979**, *20*, 1589.

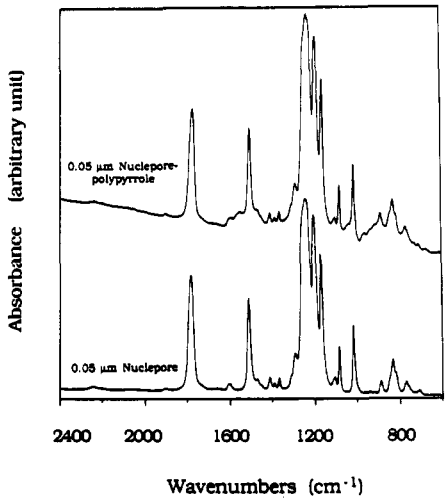

Figure 3. PIRAS data: (top) virgin Nuclepore membrane (50-nm pore diameter); (bottom) the same membrane after template synthesis of PPY fibrils and removal of the surface layers.

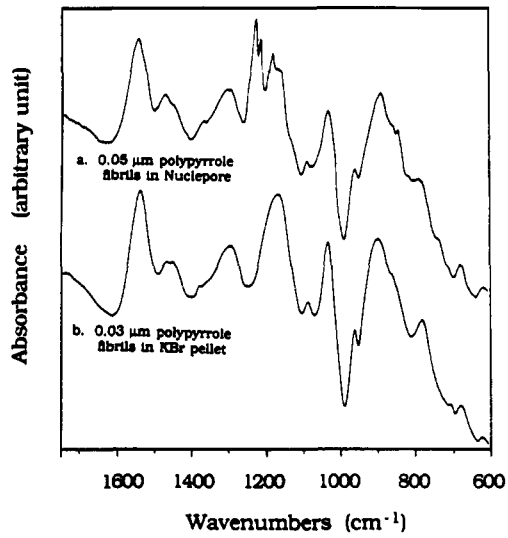

Figure 4. Top: PPY IR spectrum obtained after subtraction of background Nuclepore spectrum from composite membrane spectrum (see Figure 3). Bottom: (shown for comparison) analogous spectrum of isolated PPY fibrils in KBr pellet.

of conductive polymers.[22-24] The limitations in the applicability of this model to conductive polymers have been discussed.[22-24]

According to the Drude model, σ_{opt} is related to the absorption coefficient α via[19]

$$\sigma_{opt} = (\alpha^2 c^2)/8\pi\omega \quad (1)$$

where c is the speed of light and ω is the frequency of light employed. The absorption coefficient can be obtained from the experimental absorbance A via

$$A = \alpha b \quad (2)$$

where b is the film thickness.

Optical conductivities were obtained for 600- and 30-nm-diameter PPY fibrils and for powderous PPY. Samples were prepared by mixing measured quantities of the isolated fibrils (or powderous polymer) with measured quantities of KBr and pressing pellets; pellets were pressed at 2×10^6 psi. Infrared absorption data were obtained on these samples by using a Mattson Galaxy 4021 FTIR. A pellet devoid of polymer served as the reference.

The relevant thickness (eq 2) for these composite (polymer plus KBr) samples is not the thickness of the pellet but rather the effective thickness of the polymer dispersed within the pellet. This effective thickness was calculated from the known weight of polymer in the pellet, the area of the pellet, and the density of PPY. Densities were obtained by pressing pellets of weighed quantities of the polymer and then measuring the volume of the resulting pellets. (KBr was not added to these pellets.) The density obtained via this method is only approximate because voids left between grain boundaries might contribute to the free volume. However, the density obtained via this method (1.44 ± 0.05 g cm^{-3}, for both fibrillar and powderous PPY) agrees well with a density of 1.48 g cm^{-3} reported by Hasegawa et al.[23]

X-ray Diffraction. Diffraction data were obtained for both powderous and fibrillar PPY samples. The fibrillar samples were obtained by dissolving the template membrane and collecting the fibrils by filtration. PPY fibrils with diameters of 30 and 400 nm were investigated. Diffraction data were obtained with a Seifert-Scintag Pad diffractometer using Cu Kα radiation.

Polarized Infrared Absorption Spectroscopy (PIRAS). PIRAS is a classical technique for investigating chain orientation in polymers.[25,26] We have recently used PIRAS to prove that the polyacetylene chains in template-synthesized polyacetylene fibrils are oriented parallel to the axes of these fibrils.[2] PIRAS data for the PPY fibrils were obtained as follows:

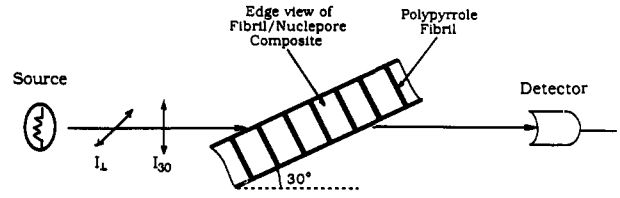

Figure 5. Configuration and polarizations used for PIRAS studies.

Prior to template synthesis, the Nucleopore membrane was placed in the FTIR sample holder, and background absorbance spectra for both polarizations employed (see below) were obtained. A typical background spectrum is shown in Figure 3 (lower curve). Template synthesis of PPY was then conducted without removing the membrane from the sample holder. (This was done so that absorbance data for the fibril/Nuclepore composite could be obtained from the same spot on the membrane used for the background spectrum.) After template synthesis, the surface PPY layers were removed by polishing with alumina powder.

The fibril/Nuclepore composite was then placed back in the spectrometer, and spectra were again obtained for each polarization. A typical composite membrane spectrum is shown in Figure 3 (upper curve). A comparison of the spectra in Figure 3 shows that the virgin Nuclepore membrane has very little absorbance at 1550 cm^{-1}, whereas the composite shows a clearly discernable peak at this energy. This peak is due to the antisymmetric ring stretching mode of the monomer units within the PPY chain.[27] While this peak appears weak (relative to the Nuclepore peaks), subtraction of the background spectrum yielded PPY spectra essentially identical with spectra obtained from the isolated fibrils (Figure 4[28]). Spectra like those shown in Figure 4 were obtained (for both of the polarizations used, see below) for PPY fibrils with diameters of 600, 400, 50, and 30 nm.

The polarizations used for the PIRAS analysis are shown in Figure 5. An Au wire grid polarizer was used to control polarization. The polarization labeled $I_\perp$ is orthogonal to the axes of the PPY fibrils. The integrated absorbance by the PPY fibrils of this polarization is labeled $A_\perp$. The polarization vector for the beam labeled I_{30} makes an angle of 30° with respect to the fibril axes. The integrated absorbance by the fibrils of this polarization

(25) Monnerie, L. In Ward, I. M., Ed. *Developments in Oriented Polymers*; Elsevier: London, 1987; Vol. 2.

(26) Zbinden, R. *Infrared Spectroscopy of High Polymers*; Academic Press: New York, 1964; p 186.

(27) Lord, R. C.; Miller, F. A. *J. Chem. Phys.* **1942**, *10*, 328.

(28) As can be seen in Figure 4, the Nuclepore membrane shows an extremely intense series of bands at ca. 1200 cm^{-1}. A vestige of this band can be seen in the background-corrected spectrum (upper curve in Figure 5) at ca. 1250 cm^{-1}. This uncorrected background peak is, however, so far removed from the 1550-cm^{-1} band used in the PIRAS analysis that its presence is not a problem.

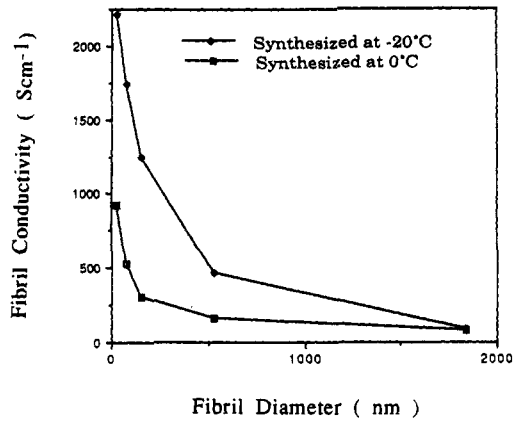

Figure 6. Plot of fibril conductivity vs. fibril diameter for PPY fibrils synthesized at two different temperatures.

Table III. Highest Dc Conductivities Obtained to Date for 30-nm-Diameter Polyheterocyclic Fibrils

polym	synth temp, °C	conductivity, Ω^{-1} cm^{-1}
PPY[a]	0	923
PPY[a]	-20	2215
PMT[b]	-20	1680

[a] Pyrrole concentration = 0.2 M; $FeCl_3$ concentration = 1 M. Solvent was 50:50 methanol/water. [b] 3-Methylthiophene concentration = 0.6 M; $Fe(ClO_4)_3$ concentration = 3 M. Solvent was acetonitrile.

is labeled A_{30}. In general, if $A_\perp = A_{30}$, the PPY chains are randomly oriented within the fibrils; nonequal integrated absorbancies indicates that the polymer chains show some preferred spatial orientation.[25,26]

The integrated absorbancies can be used to obtain a parameter called the dichroic ratio, $R = A_\parallel/A_\perp$, where $A_\parallel$ is the integrated absorbance intensity for a beam polarized parallel to the fibril axis.[29] The dichroic ratio quantitatively describes the extent of polymer chain orientation within a sample.[26,27] A_{30} is related to $A_\parallel$ and $A_\perp$ via[26]

$$A_{30} = A_\parallel \cos^2(30°) + A_\perp \sin^2(30°) \quad (3)$$

Dividing both sides of eq 3 by $A_\perp$ and rearranging yield

$$R = A_\parallel/A_\perp = \tfrac{1}{3}(4A_{30}/A_\perp - 1) \quad (4)$$

Results and Discussion

Dc Conductivity (σ_{dc}). Plots of σ_{dc} vs. fibril diameter, for fibrils synthesized at two different temperatures, are shown in Figure 6. In agreement with our previous study,[1] σ_{dc} values for the smallest fibrils increase as the fibril diameter decreases. The data in the lower curve were obtained from fibrils synthesized at 0 °C. The highest σ_{dc} achieved at this temperature was 923 S cm^{-1} (30-nm-diameter fibrils). The upper curve in Figure 6 was obtained for fibrils synthesized at -20 °C. These fibrils show conductivities dramatically higher than the fibrils synthesized at 0 °C.

Table III presents the highest conductivities obtained, to date, for 30-nm-diameter PPY and PMT fibrils. (We have not yet investigated smaller fibrils.) These data clearly illustrate the effect of synthesis temperature on σ_{dc}.[30] (The PIRAS data discussed below provide an explanation for this observation.) The 30-nm-diameter PPY fibrils synthesized at -20 °C are ca. 1 order of magnitude more conductive than the best electrochemically synthesized film.[10] Our chemically synthesized powders showed conductivities from 10 to 50 S cm^{-1}, which is typical for PMT and PPY films.[31,32]

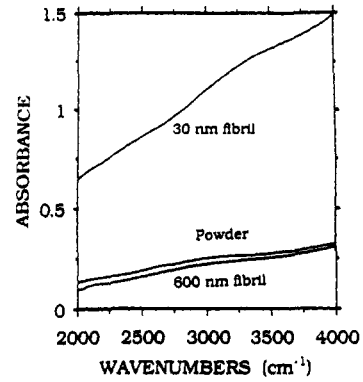

Figure 7. FTIR spectra of isolated PPY fibrils and PPY powder in KBr pellets.

Table IV. Absorption Coefficient (α, cm^{-1}) and Optical Conductivity (σ_{opt}, S cm^{-1} for PPY Fibrils and Powder[a]

energy, cm^{-1}	powder		600-nm fibril		30-nm fibril	
	α	σ_{opt}	α	σ_{opt}	α	σ_{opt}
2000	6.1×10^3	4.0	4.6×10^3	2.2	3.2×10^4	108
2500	8.7×10^3	6.4	7.7×10^3	5.1	4.3×10^4	157
3333	1.2×10^4	9.1	1.1×10^4	7.9	5.6×10^4	199
3535	1.4×10^4	12.5	1.3×10^4	9.4	6.7×10^4	271
4000	1.7×10^4	14.3	1.5×10^4	12.4	7.7×10^4	314
11000	2.7×10^4	14.9	1.9×10^4	7.0	1.8×10^5	640
12500	2.2×10^7	10.0	1.7×10^4	5.6	1.5×10^5	427

[a] All samples were synthesized at 23 °C.

Optical Conductivity (σ_{opt}). The intent of these studies was to obtain independent verification of the enhanced dc conductivities of the fibrillar polymers. IR spectra for fibrillar and powderous PPY are shown in Figure 7. These spectra show the featureless rise in absorbance with energy characteristic of PPY in this energy region.[22] All of the samples contained identical quantities of PPY; however, the absorbance for the 30-nm-diameter fibrils is significantly higher than absorbencies for the powderous material or the 600-nm-diameter fibrils. This suggests that the 30-nm-diameter fibrils are more conductive (eq 1).

Optical conductivities calculated from the IR data are shown in Table IV. In agreement with previous analyses of this type,[22] σ_{opt} increases with energy over this region (vide infra). Most importantly, note that at any frequency, σ_{opt} values for the 30-nm-diameter fibrils are over an order of magnitude higher than the corresponding σ_{opt}'s for either the 600-nm-diameter fibrils or the PPY powder. These data corroborate the dc conductivity measurements (Figure 6, Table III).

As indicated above, the objective of these experiments was to obtain corroborating evidence for the increased dc conductivities of our nanoscopic polyheterocyclic fibrils. This was accomplished by comparing optical conductivities for 30-nm fibrils with analogous σ_{opt}'s for powders and larger fibrils. Other workers have, however, attempted to make absolute comparisons between the optical and dc conductivities.[23,24] Such comparisons are, in principle,

(29) The ideal geometry would be to impinge the IR radiation on the edge of the membrane so that a truly parallel polarization vector could be achieved. Because the membranes are so thin (Table I), this configuration is impractical.

(30) Yamaura, M.; Hagiwara, T.; Hirasaka, M.; Demura, T.; Iwata, K. *Synth. Met.* **1989**, *28*, 157.

(31) Street, G. B. in *Handbook of Conducting Polymers*; Skotheim, T. A., Ed.; Marcel Dekker: New York, Vol. 1, p 282.

(32) Tourillon, G. In ref 31, p 325.

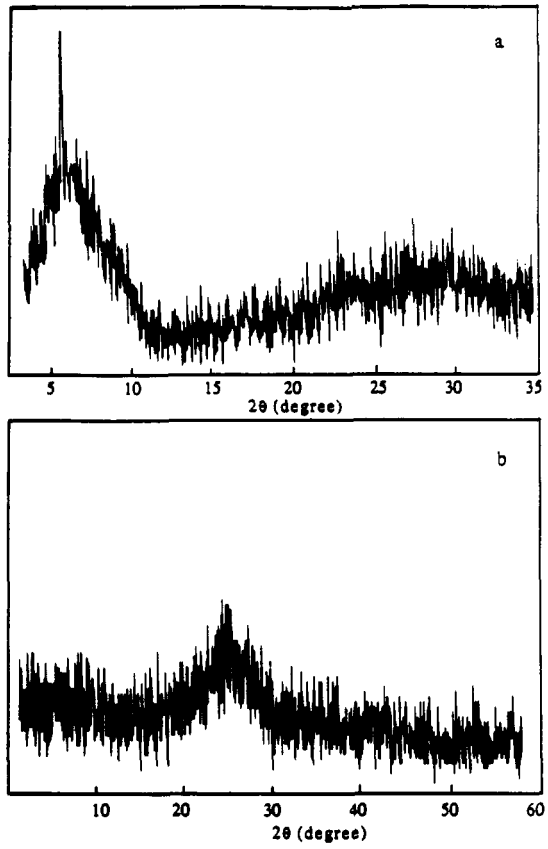

Figure 8. X-ray diffractograms for (A) 30-nm-diameter template-synthesized PPY fibrils and (B) PPY powder.

possible because the Drude model predicts that σ_{opt} is inversely proportional to frequency and approaches σ_{dc} at zero frequency.[21,24] Thus, optical and dc conductivities can, in principle, be compared by comparing $\lim_{\omega \to 0} (\sigma_{opt})$ with σ_{dc}.

We (Table IV) and others[21,22] have found, however, that PPY does not adhere to this simple Drude model prediction. (Note that σ_{opt} is proportional, rather than inversely proportional, to frequency (Table IV).) Polyacetylene shows analogous "anti-Drude" optical conductivity data.[24] This anti-Drude behavior is probably caused by defects in the polymer chains.[24] Because of this anti-Drude behavior $\lim_{\omega \to 0} (\sigma_{opt})$ is less than σ_{dc},[24] making comparison between σ_{opt} and σ_{dc} problematic. Finally, it is worth noting that the maximum absorbance for PPY is in the near-IR,[22] an energy region not accessed by this study. Evidence for this (missing) maximum can be seen in the data in Table IV. Thus, our PPY samples could show higher optical conductivities than the values presented in Table IV.

Investigations of the Supermolecular Structure. The remainder of this paper will be devoted to understanding why the nanoscopic conductive polymer fibrils show higher conductivities than electrochemically synthesized films or chemically synthesized powders. We will show here that part of this enhanced conductivity is a supermolecular effect. We will show in part 2 of this series that molecular effects also contribute to these enhanced conductivities.[8]

1. X-ray Diffraction. PPY shows a broad and very weak peak corresponding to a Bragg spacing of 0.34 nm;[30] this is usually the only feature in the diffractogram, indicating that PPY is completely amorphous. Diffractograms for our powderous PPY show only this high-angle peak (Figure 8a); diffractograms for 400-nm PPY fibrils

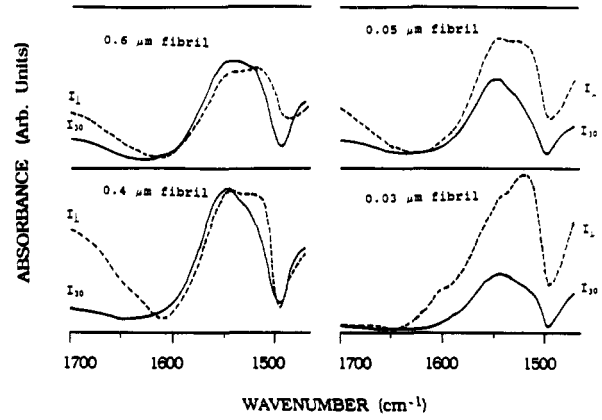

Figure 9. PIRAS spectra for PPY fibrils of various diameters.

Table V. Dichroic Ratios ($R = A_{\parallel}/A_{\perp}$) for Polypyrrole Fibrils Synthesized at Different Temperatures

	synth temp, °C	
fibril diam, μm	0	23
0.6		1.01 ● 0.04
0.4	0.95 × 0.04	0.97
0.05	0.40	0.61
0.03	0.11	0.17

are identical, indicating that these large fibrils are also completely amorphous. In contrast, diffractograms for our 30-nm-diameter PPY fibrils show a second, and more intense, peak corresponding to a Bragg spacing of 1.47 nm (Figure 8b). This new peak indicates that the polymer chains in these nanoscopic PPY fibrils show supermolecular order not present in conventional PPY.[30]

What is the nature of this enhanced order? Yamaura et al. have recently conducted X-ray diffraction analyses on stretched PPY films.[30] This stretched material also showed a low-angle peak corresponding to a Bragg spacing of ca. 1.5 nm. They suggest that stretching causes the PPY chains to align and that this alignment accounts for the new peak;[30] this is a common observation for stretch-oriented polymers.[33] The similarity between the diffraction data for stretched and template-synthesized PPY suggests that template synthesis in nanoscopic pores also causes the polymer chains to align.

This conclusion is in perfect accord with the dc conductivity data. It is well-known that aligning conductive polymer chains (typically by stretching) enhances conductivity along the alignment axis.[34] Hence, the X-ray diffraction and conductivity data suggest that the polymer chains in our narrowest fibrils are aligned parallel to the fibril axes. The PIRAS data strongly support this conclusion.

2. Polarized Infrared Absorption Spectroscopy (PIRAS). PIRAS is the ideal technique for investigating chain orientation in polymers. Typical PIRAS spectra, in the region of the PPY antisymmetric ring stretching mode, are shown in Figure 9. Note first that the large PPY fibrils (600 and 400 nm) absorb both the perpendicular and 30° polarizations to the same extent. Consequently, the dichroic ratios for these large fibrils are unity, Table V. This indicates that the polymer chains in these large fibrils show no preferred spatial orientation. This is in perfect accord with the X-ray diffraction and conductivity data for such large fibrils.

(33) Shastri, R.; Roehrs, H. C.; Brown, C. N.; Dollinger, S. E. In *Barrier Polymers and Structures*; Koros, W. J., Ed.; ACS Sym. Ser. No. 423; American Chemical Society: Washington, DC, 1990; p 240.
(34) Kirppka, M.; Doi, T. *Synth. Met.* **1987**, *17*, 209.

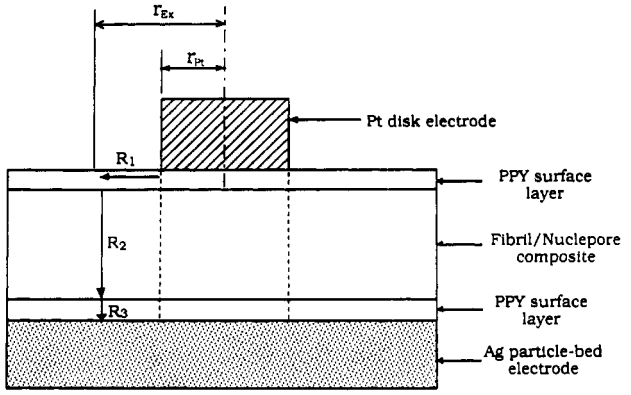

Figure 10.

In contrast, the narrow (30 and 50 nm) PPY fibrils preferentially absorb the perpendicular polarization (Figure 9). The dichroic ratios obtained from these spectra are shown in Table V; these nonunity dichroic ratios indicate that the polymer chains in these extremely narrow fibrils show a preferred spatial orientation. Furthermore, the extent of dichroism is higher in the 30-nm fibrils than in the 50-nm fibrils (Table V). This suggests that the polymer chains in the 30-nm fibrils are more strongly oriented than in the 50-nm fibrils. This is in perfect accord with the conductivity data (Figure 6; note that the 30-nm fibrils are more conductive) and the X-ray diffraction data.

As indicated in Figure 6 and Table III, PPY fibrils synthesized at −20 °C are more conductive than PPY fibrils synthesized at 0 °C. PIRAS provides a partial[30] explanation for this observation. As shown in Table V, the nanoscopic fibrils synthesized at lower temperatures show greater dichroism than analogous fibrils synthesized at higher temperature. These data suggest that the fibrils synthesized at the lower temperature are more strongly oriented; this enhanced orientation makes these low-temperature fibrils more conductive.

The conductivity, X-ray diffraction, and PIRAS data all tell a coherent story about our template-synthesized polyheterocyclic fibrils: These various data suggest that the polymer chains in the narrowest fibrils are preferentially oriented parallel to the fibril axis and that the extent of orientation increases as the diameter of the fibril and the synthesis temperature decrease.

Conclusions

An important question remains to be answered: Why is preferential polymer chain orientation "self-assembled" into the narrowest template-synthesized fibrils? While we have formulated several possible models to answer this question, we are not yet satisfied with any of these putative models. We believe, however, that polymer chain adsorption to the walls of the pore plays an important role.

In our previous communications we have shown that, during template synthesis, the nascent PPY preferentially nucleates on the pore walls of the Nuclepore membrane.[1,3] Indeed, if the reaction is quenched at short polymerization times, polymer tubules are obtained.[1,3] Kuhn et al. have observed an analogous adsorption phenomenon and have used this adsorption to prepare PPY-coated fabrics (e.g., polyester, cotton).[35] Hence, as pointed out by one of the reviewers of this paper, the enhanced conductivity observed in our fibrils may result from a surface layer of highly oriented (and thus highly conductive) material. We are currently investigating this possibility.

(35) Gregory, R. V.; Kimbrel, W. C.; Kuhn, H. H. *Synth. Met.* **1989**, *28*, C823.

Acknowledgment. This work was supported by the Office of Naval Research.

Appendix A. Effect of Surface Layers

We first show that the PPY surface layer does not contribute to the measured resistance *across* the fibril/Nuclepore composite. The conductivity of the PPY surface layer covering a fibril/Nuclepore composite membrane (30-nm-diameter pores) was measured by using the standard four-point method. A surface layer conductivity (σ_s) of 17 S cm^{-1} was obtained. (This conductivity was based on a surface layer thickness of 200 nm.) The resistance across the surface layer (R_s) can be calculated via

$$R_s = d_s/(\sigma_s A_{Pt}) \qquad \text{(A1)}$$

where d_s is the surface layer thickness (200 nm), and A_{Pt} is the area of the upper Pt electrode (0.002 cm^2). An R_s value of 6×10^{-4} Ω is obtained. This is less than 1% of the smallest experimental membrane resistance shown in Table II. Thus, the surface layers do not contribute to the resistance measured across the fibril/Nuclepore composite.

We next show that we are justified in using the area of the upper Pt disk electrode to calculate the fibril conductivity. Note first that the area of the Pt electrode is significantly smaller than the area of the lower Ag particle electrode (Figure 1). It is, therefore, in principle possible that the "real" measurement area (i.e., the area in the membrane through which current flows during the resistance measurement) is larger than the area of the upper Pt disk. We will show below that this is not the case for the composite membranes investigated here.

Consider the diagram shown in Figure 10. By assuming that the Pt disk electrode area (defined by the radius of the Pt electrode, r_{Pt} = 0.025 cm) is the relevant measurement area, we are, in essence, assuming that all of the current flows in the cylinder defined by the dashed lines in Figure 10. In fact, this will *always be true* when the radius of the electrode (0.025 cm) is much greater than the thickness of the film (7 μm). This is particularly true for the composite membranes investigated here.

Consider a hypothetical current line that flows outside of the cylinder defined by the area of the Pt disk electrode. This current must pass *laterally along* the PPY surface layer (this resistance is defined as R_1 in Figure 10), through the fibril/Nuclepore composite (resistance R_2 in Figure 10), and then through the lower PPY surface layer (R_3). The total resistance experienced by this current line then is $R_t = R_1 + R_2 + R_3$. We will consider only the resistance R_1, and we will show that this resistance is much larger than the experimental membrane resistances (Table II), indicating that the current through the hypothetical path in Figure 10 is negligibly small.

Obviously R_1 will increase linearly with the lateral distance the current travels through the PPY surface layer. We will begin by assuming that this distance is very small so as to minimize R_1 and thus maximize the probability that this current path will contribute to the total measured current. Let us assume that the length of the current path associated with R_1 is 0.001 25 cm; i.e., we are assuming that r_{ex} in Figure 10 is 0.026 25 cm. This would make the radius associated with the "real" measurement area 5% larger than the radius of the Pt disk electrode (r_{Pt} = 0.025 cm). The resistance R_1 (Figure 10) can then be approximated by (units are shown in parentheses)

$$R_1 = \frac{0.00125\ (\text{cm})}{[17\ (\Omega^{-1}\ \text{cm}^{-1})]2\pi[0.02625\ (\text{cm})][2 \times 10^{-5}\ (\text{cm})]} = 22\ \Omega$$

This R_1 is over 50 times larger than the largest measured membrane resistance (Table II). This indicates that negligible current flows through the path indicated in Figure A1.

One could lower R_1 by making the lateral current path in Figure 10 smaller. However, this would make r_{ex} approximately equal to r_{Pt} (Figure 10) and thus the "real" measurement area would be the area of the Pt disk.

Appendix B. Calculation of the Fibril Conductivity

The apparatus shown in Figure 1 provides the bulk resistance of the composite membrane, R_m, which is given by

$$1/R_m = 1/R_f + 1/R_p \quad \text{(B1)}$$

where R_f is the parallel sum of the resistances of the conductive polymer fibrils and R_p is the resistance of the intervening template membrane. Resistance measurements on virgin Nuclepore membranes show that $R_p \gg R_f$. Thus, eq 1 becomes

$$1/R_m = 1/R_f = n/R_i \quad \text{(B2)}$$

where n is the number of fibrils in the measurement area and R_i is the resistance of an individual fibril.

The number of fibrils in the measurement area can be obtained from the data in Table I and the known area of the Pt disk electrode. Thus R_i can be calculated from R_m (eq B2). R_i and the area (A) and length (l) of the fibril (Table I) can be used to calculate the fibril conductivity (σ_{fib}):

$$\sigma_{fib} = l/R_i A \quad \text{(B3)}$$

The above analysis assumes that conductive polymer grows only in the pores and not within the bulk polymer. To test this assumption, we attempted to grow polypyrrole within nonporous polycarbonate sheet. No evidence for PPY growth within the nonporous sheet was obtained, and the resistance of these sheets remained essentially infinite.

Clusters of Immiscible Metals. Iron–Lithium Nanoscale Bimetallic Particle Synthesis and Behavior under Thermal and Oxidative Treatments

George N. Glavee, Carl F. Kernizan, Kenneth J. Klabunde,* Christopher M. Sorensen, and George C. Hadjapanayis

Departments of Chemistry and Physics, Kansas State University, Manhattan, Kansas 66506, and Department of Physics and Astronomy, University of Delaware, Newark, Delaware 19716

Received February 12, 1991. Revised Manuscript Received June 10, 1991

Iron and lithium atoms have been trapped in cold, frozen pentane. Upon warming, atom agglomeration took place to form Fe–Li clusters/particles that incorporated some fragments of the organic solvent. At room temperature very small α-Fe crystallites embedded in a matrix of nanocrystalline Li were obtained. Particle sizes averaged 21 nm with α-Fe crystallite regions of about 2.8–3.8 nm. This ultrafine powder (140 m^2/g surface area) was pyrophoric. Upon allowing slow air exposure, particle growth took place and surface area dropped. However, α-Fe crystallites remained. Rapid air exposure caused intense heating to a dull red heat due to oxidation. Surprisingly, α-Fe particles remained as dominant and were encapsulated and protected from further oxidation by a $Li_2O/LiOH/Fe_2O_3$ coating. Heat treatment of the fresh Fe–Li powder caused phase separation of Fe and Li, with α-Fe crystallite growth. Air oxidation again formed a protective outer layer of $Li_2O/LiOH/Fe_2O_3$. By choice of proper temperature and time of heating the α-Fe crystallite sizes could be controlled. However, upon longer term heating at 470 °C, significant amounts of Fe_3C formed due to α-Fe crystallites reacting with carbonaceous fragments from the pentane solvent. Heating to even higher temperature then caused Fe_3C decomposition to larger α-Fe crystallites and carbonaceous species. Characterization methods included Mossbauer, X-ray powder diffraction, surface area measurements, electron microscopy, elemental analyses, X-ray photoelectron spectroscopy, and differential scanning calorimetry. These results demonstrate, for the first time, that normally immiscible metals can be forced to form metastable clusters by using low-temperature, kinetic growth control methods. Also, the isolation of encapsulated, protected α-Fe and Fe_3C nanoscale particles is a significant finding vis-à-vis new magnetic materials.

Introduction

In recent years we have witnessed a revolution in the synthesis of new materials, especially dealing with ultrafine particles (clusters) of metallic, semiconductor, and insulator materials.[1-3] The likelihood of these new materials being technologically important is very great, especially in the fields of catalysis, magnetics, adsorbents, and photovoltaic cells.

We have been interested for some time in the preparation of new bimetallic particles, which sometimes have shown interesting catalytic properties.[4-6] As an extension of this work, we have turned our attention to magnetic materials[7] and herein report some work on a bimetallic combination of iron and lithium.

To force the combination of metal atoms of two normally immiscible metals, such as Fe and Li,[8] our approach is to use atom clustering at low temperature. In this way kinetic

* To whom correspondence should be sent at the Chemistry Department, Kansas State University.

(1) Andres, R. P.; Averback, R. S.; Brown, W. L.; Brus, L. E.; Goddard, W. A.; Kaldor, A.; Louis, S. G.; Moskovits, M.; Peercy, P. S.; Riley, S. J.; Siegel, R. W.; Spaepan, F.; Wang, Y. *J. Mater. Res.* **1989**, 704.

(2) Steigerwald, M.; Alivisotas, A. P.; Gibson, J. M.; Harris, T. D.; Kortan, R.; Mueller, A. J.; Thayer, A. M.; Duncan, T. M.; Douglass, D. C.; Brus, L. E. *J. Am. Chem. Soc.* **1988**, *110*, 3046.

(3) Gesser, H. D.; Goswami, P. C. *Chem. Rev.* **1989**, *89*, 765.

(4) Klabunde, K. J.; Tanaka, Y. *J. Mol. Catal.* **1983**, *21*, 57.

(5) Tan, B. J.; Klabunde, K. J.; Tanaka, T.; Kanai, H. Yoshida, S. *J. Am. Chem. Soc.* **1988**, *110*, 5951.

(6) Tan, B. J.; Klabunde, K. J.; Sherwood, P. M. A. *Chem. Mater.* **1990**, *2*, 186.

(7) Kernizan, C.; Klabunde, K. J.; Sorensen, C. M.; Hadjapanayis, G. C. *Chem. Mater.* **1990**, *2*, 70.

(8) Moffat, W. G. *The Handbook of Binary Phase Diagrams*; Genium Publishing: Schenectady, NY, 1986; Vol. III.

0897-4756/91/2803-0967$02.50/0